

SIMULATION AND CALCULATION OF THE CONTRIBUTION OF HYPERPOLARIZATION-ACTIVATED CYCLIC NUCLEOTIDE-GATED CHANNELS TO ACTION POTENTIALS

Liping Liao¹, Xianguang Lin¹, Jieli Hu², Xin Wu², Xiaofei Yang¹, Wei Wang² and Chenhong Li^{1*}

¹ *Laboratory of Membrane Ion Channels and Medicine, Key Laboratory of Cognitive Science, State Ethnic Affairs Commission, College of Biomedical Engineering, South-Central University for Nationalities, Wuhan 430074, China*

² *Academic Affairs Office of Hubei Polytechnic University, Huangshi, Hubei, P. R. China*

*Corresponding author: lichen@mail.scuec.edu.cn

Received: April 16, 2015; **Revised:** July 15, 2015; **Accepted:** August 8, 2015; **Published online:** December 29, 2015

Abstract: The hyperpolarization-activated cyclic nucleotide-gated (HCN) channel, which mediates the influx of cations, has an important role in action potential generation. In this article, we describe the contribution of the HCN channel to action potential generation. We simulated several common ion channels in neuron membranes based on data from rat dorsal root ganglion cells and modeled the action potential. The ion channel models employed in this paper were based on the Markov model. After modifying and calibrating these models, we compared the simulated action potential curves under the presence and absence of an HCN channel and calculated that the proportional contribution of the HCN channel in the potential recovery phase was 33.39%. This result indicates that the HCN channel is critical in assisting membrane potential recovery from a hyperpolarized state to a resting state. Furthermore, we showed how the HCN channel modifies the firing of the action potential using mathematic modeling. Our results indicated that although the loss of the HCN channel made recovery of the membrane potential more difficult from the most negative point to resting in comparison with the control, the firing rate of the action potential increased in certain circumstances. We present a novel explanation for the HCN channels' mechanism in neuron action potential generation using mathematical models.

Key words: HCN channel; action potential; mathematical model; simulation and calculation; dorsal root ganglion

INTRODUCTION

The action potential in a dorsal root ganglion cell is formed under the contributions of a number of ion channels, and these ion channels seek a dynamic equilibrium, which forms a sine-wave-like signal (Schulz, 2006; Turrigiano, 2008). Hyperpolarization-activated cyclic nucleotide-gated cation (HCN) channels are open when the membrane potential becomes hyperpolarized. HCN channels help the membrane potential recover from the hyperpolarized phase to resting as a "pacemaker", and the neuron easily accepts another stimulation and cycles through action potential firing (Magee, 1998; Wahl-Schott and Biel, 2009). However, it is complicated to measure the precise con-

tribution of HCN channels using a patch clamp due to the mixed channel signal in a living cell. Here, we used a mathematical model to calculate the contribution of HCN channels to the action potential in dorsal root ganglion (DRG) cells. Mathematical simulations are very powerful in research as they can help us to avoid the defects of *in vivo* experiments. Also, researchers can use simulations to predict possible results and to create a reference for upcoming work. Our results showed that HCN channels provided approximately 1/3 of inward nerve currents. In addition, by applying this model we found a reasonable explanation for the priming effect of the downregulation of HCN expression in action potential generation.

MATERIALS AND METHODS

Animals and electrophysiology

Animal studies conformed to the Guide for the Care and Use of Laboratory Animals of the National Institutes of Health and were approved by the Institutional Animal Care and Use Committee at the South-Central University for Nationalities.

DRG neuron cells were isolated as described by Wu et al. (2012). Briefly, Wistar rats (approximately 200 g) were sacrificed by cervical dislocation; then the L4-L6 DRGs were minced and digested by collagenase (2.5 mg/mL, type I, Invitrogen) and trypsin (1.25 mg/mL, Invitrogen) for 10-15 min at 37°C. After the reaction was stopped by the addition of the culture medium containing 10% fetal bovine serum (FBS), the cells were collected by gentle centrifugation (approximately 800-1000 rpm) and used for the recording. Patch clamp experiments were carried out after 2-3 h at room temperature. HCN channel current data were obtained from DRG cells in adult Wistar rats using Axopatch 700B (Axon Instruments, USA). The output was sampled at 20 kHz and filtered at 5 kHz. For whole cell action potential recording, a pipette was modified by a Sutter p97 puller and heat-polished to 3-4M Ω . For sodium channel current recording, the pipette was filled with 140 mM CsF, 10 mM NaCl, 5 mM EGTA and 10 mM HEPES (pH 7.2 with CsOH). Bath solution contained 140 mM NaCl, 5 mM D-glucose, 1 mM MgCl₂, 3 mM KCl, 1 mM CaCl₂, 10 mM HEPES (pH 7.4 with NaOH). For potassium channel current recording, the internal solution contained 140 mM KCl, 0.5 mM CaCl₂, 1 mM MgCl₂, 5 mM EGTA, 10 mM HEPES, 3 mM MgATP, and 0.3 mM Na₂GTP (pH 7.4 with KOH). The external solution contained (in): 150 mM choline-Cl, 5 mM KCl, 0.03 mM CaCl₂, 10 mM HEPES, 1 mM MgCl₂ and 10 mM glucose (pH 7.4 with KOH). For recording of HCN channel currents, the pipette solution was filled with a solution containing 135 mM KCl, 10 mM MgCl₂, 0.1 mM CaCl₂, 1 mM EGTA, 10 mM HEPES (pH 7.2 with KOH). The bath solution contained 140 mM NaCl, 5 mM KCl, 1 mM MgCl₂, 10 mM HEPES, 2 mM CaCl₂, 10 mM D-glucose (pH 7.4 with NaOH). For action

potential recording, the pipette was filled with 140 mM KCl, 0.5 mM EGTA, 5 mM HEPES, and 3 mM Mg-ATP, 10 mM D-glucose (pH 7.30 with KOH), and the bath solution contained 140 mM NaCl, 3 mM KCl, 2 mM MgCl₂, 2 mM CaCl₂, 10 mM HEPES, 10 mM D-glucose (pH 7.30 with NaOH).

Simulation and calculation

Cell simulation software (Cel) was provided by Prof. Ding's group (Institute of Biochemistry and Biophysics, Huazhong University of Science and Technology) to for all simulation processes (Wang et al., 2012). The Cel software has three main modules: (i) voltage clamp for kinetic simulation of ion channels; (ii) current clamp for simulating the action potentials of cells, and (iii) fit-kinetics for automatically calculating the parameters of kinetic models.

To find the contribution of the HCN channels, we set up models of potassium channels, sodium channels, Ito (the transient outward K⁺ current) channels and HCN channels in the Cel software. To simulate the type of channel, we began with a 2-state model, including one open form and then we expanded it to more open form, closed form and inactivation form. The expansion included two parts: the first one was to search for the appropriate number of states, and the second was to calculate the proper transformation probability among the different states. The initial transformation parameter value was set to 1; we used the Cel software to adjust this value within a range of 0.01-100 to simulate the ion channel current. We then input the actual experimental data into the Cel software and fitted the data with the parameters to test whether they were appropriate. While establishing our model, we used an MWC/KNF model to describe each ion channel. This model can only be used on the cells with soma only, because all the data were gathered from DRG cells without synapses. After models of each ion channel were built, we combined them to generate an action potential wave using the Cel software. Then, we contrasted the parameters between the artificial action potential and the recorded action potential. According to these results, we adjusted our

model to make the generated curve more coincident to the real curve obtained by patch clamping. We drew the simulated and the real action potential curve in one graph and then calculated the area between these two curves. The smaller the area means a better simulation (Cui and Mao, 2012). Supplementary Fig. 2 shows the simulated and the recorded current curves. In general, the critical parameters were the local conductance, reversal potential and capacitance. The minimization of difference between recorded and modeled AP was the goal of our process. We selected mean absolute error and mean relative error as evaluation standards (Cui and Mao, 2012).

The mean absolute error (MAE) describes the average deviation between simulated and true values. The mean relative error (MRE) describes the average deviation degree between them, and can better reflect the advantages and disadvantages of the model.

The expressions of the MAE and the MRE are as follows:

$$MAE = \frac{1}{n} \sum_{i=1}^n |\tilde{z}_i - z_i| \Delta t_i$$

$$MRE = \frac{1}{n} \frac{\sum_{i=1}^n |\tilde{z}_i - z_i|}{\sum_{i=1}^n z_i},$$

where \tilde{z}_i represents the simulated value, z_i represents the true value, n represents test points, Δt_i represents time step, which is 0.1 ms in our model and recorded data.

Obviously, if MAE and MRE are smaller, then the error is smaller, and the simulation accuracy higher. We performed the computation in our model and the MAE and MRE are presented as follows:

$$MAE = \frac{1}{n} \sum_{i=1}^n |\tilde{z}_i - z_i| \Delta t_i = 0.7725,$$

$$MRE = \frac{1}{n} \frac{\sum_{i=1}^n |\tilde{z}_i - z_i|}{\sum_{i=1}^n z_i} = 0.0005360,$$

which shows that the value of the MAE and MRE is in a reasonable range. The value of MRE is small enough for us to believe that the simulated curve is acceptable (Supplementary Fig. 1 shows the calculated area between curves).

Data analysis

Electrophysiology data were recorded by patch clamp with voltage clamp or current clamp. Data were analyzed by Clampfit (V 10.0, Molecular Devices), SigmaPlot 10.0 and GraphPad Prism 4. Current tracing was approximated using the Runge-Kutta method.

RESULTS

Simulation of ion channel model

As shown in Fig. 1a, the overall model of the membrane channel was established. Here, we only considered the most important ion channels for action potential production, including potassium channels, sodium channels, Ito channels and, our main focus, HCN channels. Leakage was characterized as a consistently open channel on the cell membrane. In this model, two global parameters were determined first: the capacitance of the cell membrane and the resting potential (Table 1a). The mimic stimulation protocol is shown in Fig. 1b, for which the sampling frequency was 10 KHz.

In the process of simulating the action potential, it was necessary to adjust the local conductance and reverse potential of each ion channel model to bring the simulated curve closer to the real data. The final parameters used in this article are shown in Table 1b.

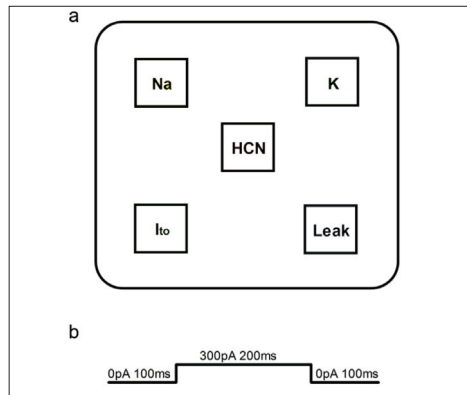


Fig. 1. Models and simulated protocol. **a** – model of membrane channels; **b** – the protocol used to generate the simulated action potential.

Table 1. Parameter values in the global and local model. **a** – the values of global parameters in the model; **b** – the local conductance and reversal potentials of each channel in the model.

Parameter	Parameter description	Values
cm (pf)	membrane capacitance	7
Resting potential (mv)	The resting membrane potential	-55

a

Parameter	Parameter description	Values
Na+	Local membrane capacitance	
g (Ns)	Local conductance of sodium channel	260
VE (mV)	Reversal potential of sodium channel	65
K+	Potassium channel model	
g (Ns)	Local conductance of potassium channel	42
VE (mV)	Reversal potential of potassium channel	-80
Ito	Ito channel model	
g (Ns)	Local conductance of Ito channel	10
VE (mV)	Reversal potential of Ito channel	-75
HCN	HCN channel model	
g (Ns)	Local conductance of HCN channel	500
VE (mV)	Reversal potential of HCN channel	0
LEAK	Leak model	
g (Ns)	Local conductance of leak	0.01
VE (mV)	Reversal potential of leak	-65

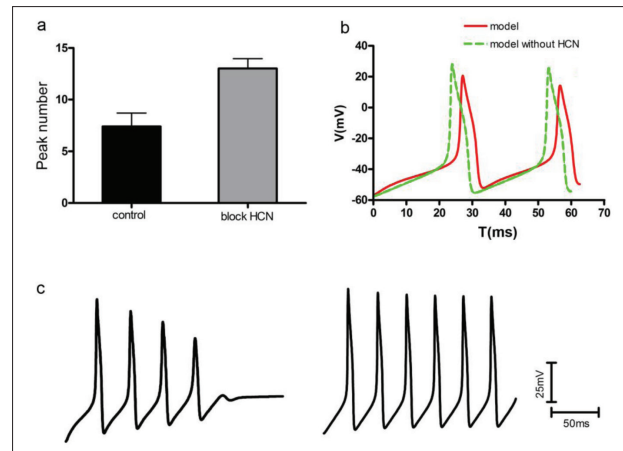


Fig. 2. Inhibition of HCN channels increased the firing possibility of action potential. **a** – number of action potentials recorded from rat DRG cells with the application of 300pA current. Blocked HCN channels (gray bar) greatly increase firing times of action potentials; **b** – in our simulation model, inhibition of HCN channels (green line) reduced the rise time from the most negative point to rest compared to the control (red line); **c** – simulation of action potential firing in our model containing HCN channels (left) and without HCN channels (right).

Sodium channel model

The sodium channel model was based on an existing model (Xiong, 2009) and was modified to make it more suitable to the actual data. We assumed that a sodium channel had 5 closed states, 5 inactivated states, an open state and a blocking state (Kuo and Bean, 1994; Raman and Bean, 2001). The rate of transition between states of similar types was proportional to sodium channel current (Douglas et al., 1967) (Fig. 2-a). The values of the parameters in Fig. 2a are shown in Table 2a.

Potassium channel model

Similar to the method of simulating the sodium channels and in accordance with the characteristics (Conforti and Millhorn, 1997; Thompson and Nurse, 1998; Conforti et al., 2000; Fearon et al., 2002) of potassium channels, we defined a model for the potassium channels. This model consisted of 5 states, including 4 closed states and 1 open state. The values of the parameters in the expression shown above and the figures are presented in Table 2b.

Transient outward potassium channel model

For transient outward potassium channels, we used a kinetic model described by Patel and Campbell (2005), from whom we obtained the specific models and parameters (Fig. 2c, Table 2c).

HCN channel model

With respect to kinetics, HCN channels and potassium channels have relatively high similarity. Thus, we first built the HCN channel model with reference to the potassium channel model. According to the characteristics of HCN channels, we designed a 5-state model containing 4 closed states and 1 open state (Fig. 2b). This model reflects the kinetics of HCN channels suitably because the simulated curve can fit the actual data well.

We then tried the model described by Altomare et al. (2001) and obtained a better simulation result. This model reflected the different states of the tetramer structure of HCN channels, including 5 closed states and 5 open states (Fig. 2d). After fitting the experimental data, we obtained the specific parameters (Table 2d). Analyzing these parameters, we found that h1 and i4 had the largest conversion probabilities among all the data, which were several times or even tens of thousands of times the values of other parameters. Hence, the conformations of the HCN channel tetramer were mainly restricted in C4 and O1 states in our model.

Leakage

Leaks were modeled as consistently open channels; thus, it was not necessary to build a specific leak model.

Simulation of action potential

As previously noted, we successfully simulated sodium channels, potassium channels, Ito channels and HCN channels and acquired several critical parameters. We then input these parameters into the Cel software to generate an action potential curve. After adjustment, we obtained a simulated action potential close to the

Table 2. Parameter values of expressions in Fig. 2a-d.

a

Parameter	Value	Parameter	Value
m	180.0	g	0.3200
n	20.10	d	0.3989
p	8.000	c	0.8000
q	20.00	u	0.7468
r	7.391	w	0.005002
s	35.02	j	2.493

b

Parameter	Value (expression)
a	$0.023 * \exp(v/22)$
b	$0.004 * \exp(-V/45)$

c

Parameter	Value	Parameter	Value
a	1.357	g	0.002932
b	34.85	h	68.94
c	0.5647	k	16.42
d	67.10	l	643.0
e	0.01322	i	91.75
f	273.0	j	47.20

d

Parameter	Value	Parameter	Value
a	0.1322	h0	0.0341
b	22.16	h1	245.8
c	0.001823	h2	36.24
d	152.5	h3	0.03082
e	2.173	h4	0.03388
f	204.3	i0	0.002732
g	0.3524	i1	15.67
h	18.06	i2	0.06800
		i3	0.007585
		i4	364.3

real one. This simulated curve was suitable for testing the electrophysiological function of HCN channels. For example, we could selectively remove the HCN channel model to identify its effect on action potential generation. Comparing the result with experiment data, we could determine whether our model and parameters were reasonable. We analyzed the action potential data generated from adult rat DRG cells. Under the same current injection stimulation (300pA), blocking of HCN channels increased the action potential firing number (Fig. 3c). This result demonstrated that the inhibition of HCN channels facilitated the generation of nerve signals

and was consistent with observations in epileptic animals (Chung et al., 2009). Although this phenomenon was difficult to explain on the cellular level, our model successfully simulated it. As shown in Fig. 3c in the model without HCN channels, we simulated a 300pA current injection for 150 ms, and obtained 4 action potentials. After we set the contribution of HCN channels to 0, the number of action potentials increased to 6. Although the net influx of cations was reduced, the action potential could be elicited by a lower potential (Fig. 3b).

The role of HCN channels in action potential hyperpolarization recovery

HCN channels are activated when the membrane potential is hyperpolarized, but their proportional contribution from the hyperpolarized phase to the resting phase remains unclear. Here, we used the slope of the recovery in the simulated curve to measure the HCN channels' contribution. If the slope reached 0 when the HCN channels were removed from the simulation model, then the contribution of the HCN channels to recovery is 100%. However, if the slope did not change after the HCN channels were removed, then the contribution of the HCN channels is 0%. As shown in Fig. 3b, removing or keeping HCN channels in our model changed the slope of recovery. Therefore, we obtained the following equation:

$$K = \frac{V_{rest} - V_{min}}{\Delta T}$$

In this equation, K is the slope of recovery; V_{rest} is the resting potential; V_{min} is the potential of the most negative point; ΔT is the time from the most negative point to the resting potential of the curve. Thus, we obtained slope K_m from the control simulated curve and K_{mwHCN} from the model curve in which the HCN channels were removed. The values of K_m and K_{mwHCN} were 1.12 and 0.746, respectively. Then, we calculated the contribution of the HCN channels from the slope ratio (G_{HCN}):

$$G_{HCN} = \left(1 - \frac{K_{mwHCN}}{K_m}\right) * 100\% = \left(1 - \frac{0.746}{1.12}\right) * 100\% \approx 33.39\%$$

DISCUSSION

HCN channels carry a mixed sodium-potassium ion current inward and play an important role in excitable tissues, such as cardiac and brain. HCN channels are activated by membrane hyperpolarization. In the generation of an action potential firing, HCN channels lead an inward membrane current following hyperpolarization, depolarizing the membrane to the threshold for the next action potential (Brown et al., 1979; Brown and DiFrancesco, 1980). However, the exact contribution of HCN channels in this depolarization progress is an open question for many reasons, such as experimental data uncertainty, interruption of the specific channel inhibitors of other channels and cell states. In this investigation, we found the slope of the curve in a mathematical model and found the contribution of the HCN channels to be 33.39%, which could be used as a reference in future experiments.

Due to their function in action potential generation, HCN channels are related to many neuron system diseases. HCN channels are key determinants of neuronal network activity (Baruscotti et al., 2010) and related to nerve system diseases, such as neuropathic pain (Emery et al., 2012), inflammatory pain (Emery et al., 2011) and epilepsy (Kase et al., 2012). Many HCN blockers or openers are being screened to cure such symptoms and one of them is already used (Postea and Biel, 2011). But there is a contradiction about the function of HCN channels. Generally speaking, at the cellular level, blocking HCN channels results in less cation flow into the cell, which makes the cell more difficult to excite (He et al., 2014). This mechanism is sufficient to explain the effect of HCN channel inhibition on neuropathic pain (Wells et al., 2007; Weng et al., 2012), but this role is contradicted by the currently accepted mechanism of epilepsy. Knocking out HCN channels from mice does not reduce the risk of seizure but causes the mice to be more prone to epilepsy (Kole et al., 2007; Kase et al., 2012). Hence, the effect of the regulation of HCN channels on cell excitability is distinct in different circumstances. Our model shows one such possibility: that the inhibition of HCN channels could make the cell more excitable and facilitate the firing of action potentials (Fig. 3).

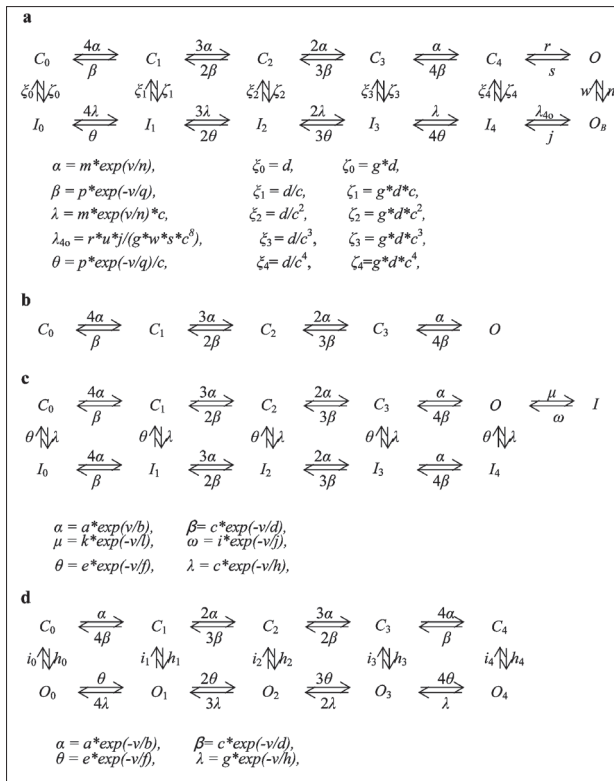


Fig. 3. Simulation models for Ion channels. **a** – simulation model of a sodium channel. C_i ($i = 0,1,2,3,4$), closed state of the sodium channel; O , open state of the sodium channel; I_i ($i = 0,1,2,3,4$), inactivated state of the sodium channel; O_B , blocked state of the sodium channel; $\alpha, \beta, \lambda, \lambda_{40}, \theta, \xi_u$ ($u = 0, 1, 2, 3, 4$), ζ_u ($u = 0, 1, 2, 3, 4$), r, s, j, n, w, s , the probability of a conversion factor; **b** – potassium channel model. C_i ($i = 0,1,2, 3$), closed state of the potassium channel; O , open state of the potassium channel. **a**, base of the potassium channel transition probability from the closed state to the open state. **b**, base of the potassium channel transition probability from the open state to the closed state; **c** – transient outward potassium channel model. C_i ($i = 0,1,2, 3$), closed state of the transient outward potassium channel; I_i ($i = 0, 1, 2, 3, 4$) and I , inactivated state of the transient outward potassium channel; O , open state of the transient outward potassium channel; $\alpha, \beta, \theta, \lambda, \mu, \omega$, rate of transition between different states of the transient outward potassium channel; **d** – HCN channel model. C_i ($i = 0, 1, 2, 3, 4$), closed state of the HCN channel; O_i ($i = 0, 1, 2, 3, 4$), e , open state of the HCN channel. $\alpha, \beta, \theta, \lambda$, rate of transition between similar states of the HCN channel; h_i ($i = 0, 1, 2, 3, 4$), rate of transition from the closed state to the open state of the HCN channel; i_i ($i = 0, 1, 2, 3, 4$), rate of transition between from various open states to various closed states of the HCN ion channel. v , variable in the model. The values of other parameters are given in Table 2.

In short, we successfully simulated action potential curves in our model, and we estimated the contribution of the action potential to hyperpolarization. We have also explained the function of HCN channels in regulating cell excitability. This model contains only sodium channels, potassium channels, Ito channels, leaks and HCN channels, which may lead to some deviation and should be expanded in future work.

Acknowledgments: This work was supported by the special funds of basic research operating expenses for universities in China [CZZ11009, CZW15048, GZY13001, CZY13012] and by the National Science Foundation of China [81271234, 30972848].

Authors' contributions: Liping Liao, Xianguang Lin, Jieli Hu calculated and simulated the HCN channel, constructed the mathematical model, wrote the paper; these authors contributed equally to the paper. Xin Wu performed the patch clamp experiment and experiments with the primary DRG cell culture. Xiaofei Yang wrote the discussion and supervised the patch clamp experiment. Wei Wang wrote the software for simulation of the HCN channel. Chenhong Li designed the whole experiment and revised the paper.

REFERENCES

Altomare, C., Bucchi, A., Camatini, E., Baruscotti, M., Viscomi, C., Moroni, A. and D. DiFrancesco (2001). Integrated allosteric model of voltage gating of HCN channels. *J Gen Physiol.* **117**, 519-532.

Baruscotti M., Bottelli, G., Milanesi, R., DiFrancesco, J.C. and D. DiFrancesco (2010). HCN-related channelopathies. *Pflugers Arch.* **460**, 405-415.

Brown, H. and D. DiFrancesco (1980). Voltage-clamp investigations of membrane currents underlying pace-maker activity in rabbit sino-atrial node. *J Physiol.* **308**, 331-351.

Brown, H. F., DiFrancesco, D. and S. J. Noble (1979). How does adrenaline accelerate the heart? *Nature.* **280**, 235-236.

Chung, W. K., Shin, M., Jaramillo, T. C., Leibel, R. L., LeDuc, C. A., Fischer, S. G., Tzilianos, E., Gheith, A. A., Lewis, A. S. and D. M. Chetkovich (2009). Absence epilepsy in apathetic, a spontaneous mutant mouse lacking the h channel subunit, HCN2. *Neurobiol Dis.* **33**, 499-508.

Conforti, L., Bodi, I., Nisbet, J. W. and D. E. Millhorn (2000). O2-sensitive K+ channels: role of the Kv1.2 -subunit in mediating the hypoxic response. *J Physiol.* **524**, 783-793.

Conforti, L. and D. E. Millhorn (1997). Selective inhibition of a slow-inactivating voltage-dependent K+ channel in rat PC12 cells by hypoxia. *J Physiol.* **502**, 293-305.

- Cui, Y. and D. Mao (2012). Error self-canceling of a difference scheme maintaining two conservation laws for linear advection equation. *Math Comput.* **81**, 715-741.
- Douglas, W. W., Kanno, T. and S. R. Sampson (1967). Influence of the ionic environment on the membrane potential of adrenal chromaffin cells and on the depolarizing effect of acetylcholine. *J Physiol.* **191**, 107-121.
- Emery, E.C., Young, G. T., Berrocoso, E. M., Chen, L. and P. A. McNaughton (2011). HCN2 ion channels play a central role in inflammatory and neuropathic pain. *Science.* **333**, 1462-1466.
- Emery, E.C., Young, G. T. and P. A. McNaughton (2012). HCN2 ion channels: an emerging role as the pacemakers of pain. *Trends Pharmacol Sci.* **33**, 456-63.
- Fearon, I. M., Thompson, R. J., Samjoo, I., Vollmer, C., Doering, L. C. and C. A. Nurse (2002). O2-sensitive K⁺ channels in immortalised rat chromaffin-cell-derived MAH cells. *J Physiol.* **545**, 807-818.
- He, C., Chen, F., Li, B. and Z. Hu (2014). Neurophysiology of HCN channels: from cellular functions to multiple regulations. *Prog Neurobiol.* **112**, 1-23.
- Kase, D., Inoue, T. and K. Imoto (2012). Roles of the subthalamic nucleus and subthalamic HCN channels in absence seizures. *J Neurophysiol.* **107**, 393-406.
- Kole, M.H., Brauer, A.U. and G.J. Stuart (2007). Inherited cortical HCN1 channel loss amplifies dendritic calcium electrogenesis and burst firing in a rat absence epilepsy model. *J Physiol.* **578**, 507-525.
- Kuo, C. C. and B. P. Bean (1994). Na⁺ channels must deactivate to recover from inactivation. *Neuron.* **12**, 819-829.
- Magee, J. C. (1998). Dendritic hyperpolarization-activated currents modify the integrative properties of hippocampal CA1 pyramidal neurons. *J Neurosci.* **18**, 7613-7624.
- Patel, S. P. and D. L. Campbell (2005). Transient outward potassium current, 'I_{to}', phenotypes in the mammalian left ventricle: underlying molecular, cellular and biophysical mechanisms. *J Physiol.* **569**, 7-39.
- Postea, O. and M. Biel (2011). Exploring HCN channels as novel drug targets. *Nat. Rev. Drug Discov.* **10**, 903-914.
- Raman, I. M. and B. P. Bean (2001). Inactivation and recovery of sodium currents in cerebellar Purkinje neurons: evidence for two mechanisms. *Biophys J.* **80**, 729-737.
- Schulz, D. J (2006). Plasticity and stability in neuronal output via changes in intrinsic excitability: it's what's inside that counts. *J Exp Biol.* **209**, 4821-4827.
- Thompson, R. J. and C. A. Nurse (1998). Anoxia differentially modulates multiple K⁺ currents and depolarizes neonatal rat adrenal chromaffin cells. *J Physiol.* **512** (Pt 2), 421-434.
- Turrigiano, G. G. (2008). The self-tuning neuron: synaptic scaling of excitatory synapses. *Cell.* **135**, 422-435.
- Wahl-Schott, C. and M. Biel (2009). HCN channels: structure, cellular regulation and physiological function. *Cell Mol Life Sci.* **66**, 470-494.
- Wang, W., Xiao, F., Zeng, X., Yao, J., Yuchi, M. and J. Ding. Optimal estimation of ion-channel kinetics from macroscopic currents. *PLoS ONE.* (2012) **7**, e35208.
- Weng, X., Smith, T., Sathish, J. and L. Djouhri (2012). Chronic inflammatory pain is associated with increased excitability and hyperpolarization-activated current (I_h) in C- but not Adelta-nociceptors. *Pain.* **153**, 900-914.
- Wells, J.E., Rowland, K.C. and E.K. Proctor (2007). Hyperpolarization-activated channels in trigeminal ganglia innervating healthy and pulp-exposed teeth. *Int. Endod. J.* **40**, 715-721.
- Wu, X., Liao, L., Liu, X., Luo, F., Yang, T. and C. Li (2012). Is ZD7288 a selective blocker of hyperpolarization-activated cyclic nucleotide-gated channel currents? *Channels (Austin).* **6**, 438-442.
- Xiong, Y (2009). Single-cell electrophysiology simulation software development and modeling and simulation of action potentials. PhD Dissertation. Department of Biophysics. Wuhan, Huazhong University of Science and Technology.

Supplementary Material (available online)

Supplementary Fig. S1. Comparison of simulated and real action potential experiment data. The grey area between the simulated and real data shows the quality of the generated curve; the smaller the area the better the simulation.

Available at: <http://serbiosoc.org.rs/sup/SupplementaryFigS1.jpg>

Supplementary Fig. S2. Comparison of Simulated and real current experiment data. Green curve showed real experiment data and red curve expressed simulated curve. **A**, voltage gated sodium channel; **b**, voltage gated potassium channel; **c**, Transient outward potassium channel; **d**, hyperpolarization-activated cyclic nucleotide-gated (HCN) channel.

Available at: <http://serbiosoc.org.rs/sup/SupplementaryFigS2.jpg>